An effective spectral collocation method for the direct solution of high-order ODEs

N. Mai-Duy*

School of Aerospace, Mechanical and Mechatronic Engineering,

The University of Sydney, NSW 2006, Australia

Submitted to *Commun. Numer. Meth. Engng*, 20/3/2005;

Resubmitted 23/8/2005; Revised 19/10/2005

*Corresponding author: Telephone +61 2 9351 7151, Fax +61 2 9351 7060, E-mail nam.maiduy@aeromech.usyd.edu.au

SUMMARY

This paper reports a new Chebyshev spectral collocation method for directly solving high-order ordinary differential equations (ODEs). The construction of the Chebyshev approximations is based on integration rather than conventional differentiation. This use of integration allows the multiple boundary conditions to be incorporated more efficiently. Numerical results show that the proposed formulation significantly improves the conditioning of the system and yields more accurate results and faster convergence rates than conventional formulations.

KEY WORDS: spectral collocation methods; high-order ordinary differential equations; multiple boundary conditions; integrated basis-functions

1 INTRODUCTION

Spectral methods are one of the principal methods of discretization for the numerical solution of differential equations. The main advantage of these methods lies in their accuracy for a given number of unknowns. For smooth problems in simple geometries, they offer exponential rates of convergence/spectral accuracy. In contrast, finite-difference and finite-element methods yield only algebraic convergence rates. The three most widely used spectral versions are the Galerkin, collocation, and tau methods. The theory and application of spectral methods are covered extensively in review articles and monographs, see for example [1-5].

High-order ODEs arise in many applications. Examples include the transverse vibration of a uniform beam that can be modelled by a fourth-order ODE; the vibrational behaviour of a ring-like structure by a sixth-order ODE [6,7]; the bending of a cylindrical barrel shell by an eighth-order ODE [8]; and the thermal instability of

a horizontal layer of a fluid heated from below under the effect of rotation and/or a magnetic field by a sixth-, eighth-, tenth- or twelfth-order ODE [9-11].

There is a relatively small literature on spectral methods for the direct solution of such high-order problems. In solving a high-order ODE without splitting it into a set of low-order ODEs, one needs to concern the treatment of multiple boundary conditions. In the context of the spectral collocation method, there are three basic approaches to implementing the multiple boundary conditions.

Conventional approach 1 (CA1): This approach modifies the basis functions to incorporate the boundary conditions, see e.g. [4]. For example, in solving the clamped-clamped-beam eigenvalue problem, one can multiply interpolating polynomials by $(1 - x^2)$; the solution procedure then becomes simple: (i) to collocate the governing equation at the interior points and (ii) to remove the first and last columns of the obtained system. However, it is difficult to apply this approach to problems involving complicated boundary conditions.

Conventional approach 2 (CA2): This approach takes fewer nodes from the data set to collocate the differential equation, see e.g. [4]. Let p be the order of a high-order ODE (also the number of boundary conditions) and $(N + 1)$ be the number of grid points. The ODE is approximated only at the $(N + 1 - p)$ points. Apart from the two boundary points, the question here is which grid points are further put aside. The performance of the spectral collocation method can depend on the choice of such points. On the other hand, the implementation of this approach is straightforward.

Conventional approach 3 (CA3): This approach uses fictitious points as additional unknowns, see e.g. [3]. A set of $(p-2)$ fictitious nodes is added to the original data set. The location of these points can be chosen arbitrarily. Since the truncated

Chebyshev series expansion can be seen as the Lagrange interpolation polynomial based on the collocation points, one can construct the Chebyshev differentiation matrices using the recurrence finite-difference formulae on arbitrarily spaced grids [3]. Like the case of second-order ODEs, the high-order ODE is forced to be satisfied exactly at the interior points. Since the unknown vector is larger, it allows one to add $(p-2)$ additional equations to the main system to impose the multiple boundary conditions. This approach requires a larger set of data points. However, it provides proper implementation of the multiple boundary conditions and overcomes difficulties encountered in the first approach.

Recently, in the context of radial-basis-function networks, a new collocation formulation based on integration for solving high-order ODEs was proposed [12]. In this study, this formulation is extended to the case of Chebyshev polynomials. The Chebyshev approximations of the dependent variable and its derivatives are constructed through an integration process; the integration constants are exploited to deal with the multiple boundary conditions. There is no need here to introduce fictitious points or to reduce the number of nodes used for collocating the ODE. The proposed Chebyshev collocation method is applicable to general high-order ODEs, where these equations can have variable coefficients, nonlinear terms, nonhomogeneous terms, complicated boundary conditions and numerous different derivatives. The method is verified through the solution of such ODEs governing initial-value, boundary-value and eigenvalue problems. Among those are the free vibration of a nonuniform ring, the free vibration of a uniform beam, and the Hamel flow problem that have a wide range of applications in engineering. Numerical results show that the proposed approach outperforms conventional approaches regarding the conditioning of the system, accuracy and convergence rate.

The remainder of the paper is organized as follows. In section 2, a brief review of the Chebyshev polynomials is given. A new Chebyshev collocation formulation based on

integration for directly solving high-order ODEs is presented in section 3. In section 4, the proposed method is verified through the solution of various problems governed by ODEs of the second-, fourth-, sixth-, eighth- and twelfth-orders. Section 5 gives some concluding remarks.

2 CHEBYSHEV POLYNOMIALS

The Chebyshev polynomial of first kind $T_k(x)$ is defined by

$$T_k(x) = \cos(k \arccos(x)), \qquad k = 0, 1, 2, \cdots, \tag{1}$$

where $-1 \leq x \leq 1$. The polynomial $T_k(x)$ can be expanded in power series as

$$T_0(x) = 1, \tag{2}$$

$$T_k(x) = \frac{k}{2} \sum_{m=0}^{[k/2]} (-1)^m \frac{2^{k-2m}(k-m-1)!}{m!(k-2m)!} x^{k-2m}, \quad k > 0, \tag{3}$$

where $[k/2]$ is the integer part of $k/2$.

3 THE SPECTRAL COLLOCATION METHOD

Consider the following ODE

$$Lu = f, \quad a \leq x \leq b, \tag{4}$$

where L is a differential operator and f is a given function. This equation is coupled with a set of prescribed conditions to constitutive the initial-value/boundary-value/eigenvalue problem. The domain of interest is represented by a set of unevenly-

spaced Gauss-Lobatto (G-L) points

$$\{x_i\}_{i=0}^{N} = \left\{ \cos\left(\frac{\pi i}{N}\right) \right\}_{i=0}^{N} \tag{5}$$

which cluster at boundaries.

3.1 Conventional differentiation-based formulations (CDFs)

An approximate solution $u(x)$ is sought in the truncated Chebyshev series form

$$u(x) = \sum_{k=0}^{N} a_k T_k(x), \tag{6}$$

where $\{a_k\}_{k=0}^{N}$ is the set of expansion coefficients to be found. The pth-order derivative of the variable u is then obtained through differentiation as

$$\frac{d^p u(x)}{dx^p} = \sum_{k=0}^{N} a_k \frac{d^p T_k(x)}{dx^p}. \tag{7}$$

The use of G-L points (5) allows a fast Fourier transform to be employed to shift between spectral space $\{a_k\}_{k=0}^{N}$ and physical space $\{u_i\}_{i=0}^{N}$:

$$a_k = \frac{2}{N\bar{c}_k} \sum_{i=0}^{N} \frac{1}{\bar{c}_i} u_i T_k(x_i), \tag{8}$$

where $\bar{c}_0 = \bar{c}_N = 2,\ \bar{c}_i = 1$ for $i = 1, 2, \cdots, N-1$.

The evaluation of the derivatives (7) at the G-L points yields

$$\widehat{\frac{du}{dx}} = \mathbf{D}^{(1)}\widehat{u} = \mathbf{D}\widehat{u}, \tag{9}$$

$$\widehat{\frac{d^2u}{dx^2}} = \mathbf{D}^{(2)}\widehat{u} = \mathbf{D}^2\widehat{u}, \tag{10}$$

$$\cdots \quad \cdots \quad \cdots \quad \cdots$$

$$\widehat{\frac{d^pu}{dx^p}} = \mathbf{D}^{(p)}\widehat{u} = \mathbf{D}^p\widehat{u}, \tag{11}$$

where the symbol $\widehat{.}$ is used to denote a vector, e.g., $\widehat{u} = (u(x_0), u(x_1), \cdots, u(x_N))^T$ and $\widehat{\frac{d^pu}{dx^p}} = \left(\frac{d^pu}{dx^p}(x_0), \frac{d^pu}{dx^p}(x_1), \cdots, \frac{d^pu}{dx^p}(x_N)\right)^T$, and $\mathbf{D}^{(.)}$ are the differentiation matrices. The entries of $\mathbf{D}$ ($\mathbf{D}^{(1)}$) are given by

$$D_{ij} = \frac{\bar{c}_i}{\bar{c}_j}\frac{(-1)^{i+j}}{x_i - x_j}, \qquad 0 \le i, j \le N, \quad i \ne j, \tag{12}$$

$$D_{ii} = -\frac{x_i}{2(1-x_i^2)}, \qquad 1 \le i \le N-1, \tag{13}$$

$$D_{11} = -D_{NN} = \frac{2N^2+1}{6}. \tag{14}$$

As an alternative approach, the diagonal entries of $\mathbf{D}$ can be computed in the way that represents exactly the derivative of a constant [13]

$$D_{ii} = -\sum_{j=0, j\ne i}^{N} D_{ij}. \tag{15}$$

Higher-order derivatives $\mathbf{D}^{(p)}$ can be constructed using recursions, see e.g. [3,14], which are faster and more numerically stable. The roundoff properties of the spectral differentiation matrices were studied in, e.g., [13,15].

Using the above expressions, the ODE can be transformed into a set of algebraic equations. The multiple boundary conditions are imposed by using the CA2/CA3

that was briefly reviewed earlier. The obtained system is then solved for the values of the variable u at the grid points. There are a number of software packages implementing spectral methods. Among them are MATLAB packages by Trefethen [4] and Weideman and Reddy [16]. The former and Fornberg's recursion codes used for finding finite-difference weights on arbitrarily spaced grids [3] are employed in the present work for calculating the CDF case.

3.2 The proposed integration-based formulation (PIF)

For the proposed formulation, the highest-order derivative $d^p u/dx^p$ in the differential equation is sought in the truncated Chebyshev series form

$$\frac{d^p u(x)}{dx^p} = \sum_{k=0}^{N} a_k T_k(x). \tag{16}$$

Expressions for lower derivatives and the variable itself are then obtained through integration as

$$\frac{d^{p-1} u(x)}{dx^{p-1}} = \sum_{k=0}^{N} a_k I_k^{(p-1)}(x) + c_1, \tag{17}$$

$$\frac{d^{p-2} u(x)}{dx^{p-2}} = \sum_{k=0}^{N} a_k I_k^{(p-2)}(x) + c_1 x + c_2, \tag{18}$$

$$\cdots \quad \cdots \qquad \cdots \qquad \cdots \qquad \cdots$$

$$\frac{du(x)}{dx} = \sum_{k=0}^{N} a_k I_k^{(1)}(x) + c_1 \frac{x^{p-2}}{(p-2)!} + c_2 \frac{x^{p-3}}{(p-3)!} + \cdots c_{p-2} x + c_{p-1}, \tag{19}$$

$$u(x) = \sum_{k=0}^{N} a_k I_k^{(0)}(x) + c_1 \frac{x^{p-1}}{(p-1)!} + c_2 \frac{x^{p-2}}{(p-2)!} + \cdots c_{p-1} x + c_p, \tag{20}$$

where $I_k^{(p-1)}(x) = \int T_k(x)dx$, $I_k^{(p-2)}(x) = \int I_k^{(p-1)}(x)dx, \cdots, I_k^{(0)}(x) = \int I_k^{(1)}(x)dx$, and $c_1, c_2, \cdots, c_p$ are integration constants. These integrals can be determined by

using recurrence relations [5]

$$\int T_0(x)dx = T_1(x), \tag{21}$$

$$\int T_1(x)dx = \frac{1}{4}\left[T_0(x) + T_2(x)\right], \tag{22}$$

$$\int T_k(x)dx = \frac{1}{2}\left[\frac{T_{k+1}(x)}{(k+1)} - \frac{T_{k-1}(x)}{(k-1)}\right], \qquad k > 1, \tag{23}$$

or integrating (2)-(3) directly, e.g., for $k > 0$:

$$I_k^{(p-1)}(x) = \int T_k(x)dx = \frac{k}{2}\sum_{m=0}^{[k/2]}(-1)^m \frac{2^{k-2m}(k-m-1)!}{m!(k-2m+1)!}x^{k-2m+1}, \tag{24}$$

$$I_k^{(p-2)}(x) = \int I_k^{(p-1)}(x)dx = \frac{k}{2}\sum_{m=0}^{[k/2]}(-1)^m \frac{2^{k-2m}(k-m-1)!}{m!(k-2m+2)!}x^{k-2m+2}, \tag{25}$$

$$\cdots \quad \cdots \qquad \cdots \qquad \cdots \qquad \cdots$$

$$I_k^{(0)}(x) = \int I_k^{(1)}(x)dx = \frac{k}{2}\sum_{m=0}^{[k/2]}(-1)^m \frac{2^{k-2m}(k-m-1)!}{m!(k-2m+p)!}x^{k-2m+p}. \tag{26}$$

It can be seen that apart from the Chebyshev coefficients $\{a_k\}_{k=0}^N$, the PIF ((16)-(20)) produces new coefficients (integration constants $\{c_i\}_{i=1}^p$) whose number is equal to the order of ODE/the number of boundary conditions, i.e. p. As a result, it allows one (i) to approximate the ODE at the whole set of G-L points and (ii) to add p additional equations to the main system to impose p boundary conditions. In this sense, the PIF makes the implementation of these two parts of the solution procedure independent of each other for any order of ODE.

The evaluation of (16)-(20) at the G-L points leads to

$$\widehat{\frac{d^p u}{dx^p}} = \mathbf{T}\widehat{s} = \mathbf{I}^{(p)}\widehat{s}, \tag{27}$$

$$\widehat{\frac{d^{p-1} u}{dx^{p-1}}} = \mathbf{I}^{(p-1)}\widehat{s}, \tag{28}$$

$$\cdots \quad \cdots \quad \cdots$$

$$\widehat{\frac{du}{dx}} = \mathbf{I}^{(1)}\widehat{s}, \tag{29}$$

$$\widehat{u} = \mathbf{I}^{(0)}\widehat{s}, \tag{30}$$

where $\widehat{s} = (a_0, a_1, \cdots, a_N, c_1, c_2, \cdots, c_p)^T$ and $\mathbf{I}^{(p-1)}, \mathbf{I}^{(p-2)}, \cdots, \mathbf{I}^{(0)}$ are the known integration matrices. For convenience of computation, $\mathbf{I}^{(p)}, \mathbf{I}^{(p-1)}, \cdots, \mathbf{I}^{(1)}$ are augmented using zero-submatrices so that they have the same dimension as $\mathbf{I}^{(0)}$.

From (9)-(11) and (27)-(30), it can be seen that the CDF and PIF have similar discrete approximation forms ($\mathbf{D} \Leftrightarrow \mathbf{I}$ and $\widehat{u} \Leftrightarrow \widehat{s}$). Thus, the process of reducing the differential equation to a set of algebraic equations by the PIF is similar to that by the CDF. A distinct difference between the two formulations in implementation is that imposition of the multiple boundary conditions is conducted by means of integration constants ($\widehat{s}$ is larger than $\widehat{u}$) for the PIF and by the node-reduction/fictitious-point technique for the CDF. Both formulations result in dense system matrices of similar size.

4 NUMERICAL RESULTS

In the following examples, the accuracy of a numerical solution produced by an approximation scheme is measured via the discrete relative L_2 error defined as

$$N_e = \sqrt{\frac{\sum_{i=0}^{N} [u_e(x_i) - u(x_i)]^2}{\sum_{i=0}^{N} u_e(x_i)^2}}, \tag{31}$$

where u_e and u are the exact and approximate solutions, respectively. Nonlinear systems of equations are solved using the Picard-type and Newton-type iteration schemes. It is noted that the former is relatively easy to implement, but its convergence is often slow.

4.1 Second-order boundary-value problem

The PIF is first tested through the solution of the following second-order ODE

$$\frac{d^2u}{dx^2}+\sin(x)\frac{du}{dx}+\exp(x)u = -16\pi^2\sin(4\pi x)+4\pi\sin(x)\cos(4\pi x)+\exp(x)\left[2+\sin(4\pi x)\right], \tag{32}$$

defined over $-1 \leq x \leq 1$ and subject to the Robin boundary conditions

$$u(\pm 1) + \frac{du(\pm 1)}{dx} = 2 + 4\pi.$$

The exact solution can be verified to be $u_e = 2 + \sin(4\pi x)$. Seven data sets, $\{10, 15, \cdots, 40\}$ G-L points, are employed to study this problem. The Robin boundary conditions are imposed explicitly by adding two additional equations to the main system. Results concerning the conditioning and the discrete relative L_2 error obtained by the CDF and PIF are shown in Table 1. For the former, two versions of computing $\mathbf{D}^{(2)}$ are employed. The first version denoted by CDF1 uses the for-

mula $\mathbf{D}^{(2)} = \mathbf{D}^2$, while the second one (CDF2) uses the explicit expression of $\mathbf{D}^{(2)}$ [5]. The relative L_2 errors obtained by CDF1 and CDF2 are "exactly the same" for $(N+1) = \{10, 15, \cdots, 30\}$, but different for $(N+1) = \{35, 40\}$. In terms of accuracy, the PIF produces more accurate results than the CDFs; for example, at $(N+1) = 30$, N_es are 1.54×10^{-11} (PIF) and 4.71×10^{-8} (CDF1,2). In terms of the conditioning of the system, the PIF yields at least two orders of magnitude lower than the CDFs; furthermore, when $(N+1)$ increases from 10 to 40, the condition number increases from 2.08×10^3 to 1.30×10^6 for the CDFs, but only from 5.30×10^1 to 9.41×10^1 for the PIF. Exponential rates of convergence are achieved for both formulations. The order of the error, which is defines as $N_e = O(N^{-\alpha})$, at the first six sets is $O(N^{-21.58})$ for the PIF and $O(N^{-18.62})$ for the CDF1; the PIF case yields faster convergence.

For the CDF case, if one tries to add an algebraic polynomial $(c_1 x + c_2)$ to (6) in order to have similar forms as the PIF case, i.e.,

$$u(x) = \sum_{k=0}^{N} a_k T_k(x) + c_1 x + c_2, \tag{33}$$

$$\frac{du}{dx} = \sum_{k=0}^{N} a_k \frac{dT_k(x)}{dx} + c_1, \tag{34}$$

$$\frac{d^2u}{dx^2} = \sum_{k=0}^{N} a_k \frac{d^2T_k(x)}{dx^2}, \tag{35}$$

the obtained system of equations is singular because the first and last two columns of matrices $\mathbf{D}^{(2)}$ and $\mathbf{T}$ are identical.

4.2 Fourth-order problems

4.2.1 Initial-value problem

Consider the following fourth-order initial-value problem

$$(x^3 - 3x^2 + 6x - 6)\frac{d^4u}{dx^4} - x^3\frac{d^3u}{dx^3} + 3x^2\frac{d^2u}{dx^2} - 6x\frac{du}{dx} + 6u = 0, \quad -1 \le x \le 1, \quad (36)$$

$$\text{Initial conditions:} \quad u(-1),\ \frac{du(-1)}{dx},\ \frac{d^2u(-1)}{dx^2},\ \frac{d^3u(-1)}{dx^3},$$

$$\text{Exact solution:} \quad u_e = \exp(x) + 5x^3 - 2x^2 + x.$$

The initial values are obtained using the exact solution. Six data sets, $\{4, 6, \cdots, 14\}$ G-L points, are employed. For the CDF case, the three derivative initial conditions are enforced explicitly by adding three additional equations to the main system. It is difficult to apply the approach CA1 to this problem; only the two approaches CA2 and CA3 are employed here. Results concerning the condition number and accuracy obtained by the proposed and conventional approaches are given in Table 2. The PIF significantly improves the conditioning of the system over the CDFs, e.g., 2 orders of magnitude for the coarsest grid and 5 orders of magnitude for the finest grid. Furthermore, the PIF yields the most accurate results, followed by the CA3 and then CA2; for example, at $(N+1) = 12$, N_es are 2.13×10^{-15}, 5.92×10^{-12} and 2.15×10^{-8}, respectively. The results of the CA2 are less accurate (a few orders of magnitude greater), probably due to the fact that the ODE is not approximated at every interior point. On the other hand, all approaches feature exponential rates of convergence. The orders of the relative L_2 error measured at $(N+1) = \{6, 8, 10, 12\}$ are $O(N^{-24.32})$, $O(N^{-20.52})$ and $O(N^{-16.29})$ for the PIF, CA3 and CA2, respectively; the PIF provides faster convergence.

4.2.2 Boundary-value problem - Hamel flow problem

A steady-state two-dimensional flow in the region between two semi-infinite plane walls set at an angle 2α is known as the Hamel flow problem [17]. It is convenient to use polar co-ordinates (r, θ) where r is measured from the intersection of the two walls and θ is measured from the centreline of the duct. The inward flow, which is driven by a steady line sink at the apex, is assumed to be purely radial along the lines θ=constant ($-\alpha \leq \theta \leq \alpha$). Since the stream function ψ depends only on θ, the dimensionless governing equation for the Hamel flow can be written as

$$\frac{d^4\psi}{d\theta^4} + 4\frac{d^2\psi}{d\theta^2} - 2Re\frac{d\psi}{d\theta}\frac{d^2\psi}{d\theta^2} = 0, \tag{37}$$

subject to the boundary conditions

$$\psi(\pm\alpha) = \pm 1, \quad \text{and} \quad \frac{d\psi(\pm\alpha)}{d\theta} = 0,$$

where Re is the Reynolds number. For creeping flow ($Re = 0$) and viscous flow with very large values of Re, they can be solved analytically and their solutions are given by

$$\frac{u_r(\theta)}{u_r(0)} = \frac{\cos(2\theta) - \cos(2\alpha)}{1 - \cos(2\alpha)} \quad (Re = 0), \tag{38}$$

$$\frac{u_r(\theta)}{u_r(0)} = 3\tanh^2\left[(0.5\alpha Re)^{0.5}\,(1 - |\theta|/\alpha) + \tanh^{-1}(2/3)^{0.5}\right] - 2 \quad (Re \gg), \tag{39}$$

where u_r is the radial velocity defined as $u_r = -\frac{1}{r}\frac{\partial\psi}{\partial\theta}$. More details can be found in [17].

The domain of interest is $\theta \in [-\alpha, \alpha] = [-\pi/6, \pi/6]$. For creeping flow, six data sets, $\{5, 7, \cdots, 15\}$ G-L points, are employed. The conditioning and accuracy obtained by the PIF and CDFs are given in Table 3. Some remarks on the performance of the two

formulations are similar to the previous problem. For viscous flow, this fourth-order ODE is nonlinear and hence must be solved iteratively. The nonlinearity is handled here using trust-region methods that retain two attractive features, namely rapid local convergence of the Newton iteration scheme and strong global convergence of the Cauchy method [18]. It is noted that Newton's method can run into difficulties if the starting point is far from the solution and the Jacobian matrix is ill-conditioned. A range of $Re = \{0, 10, 50, 100, 1000, 5000\}$ is considered. The computed solutions at the lower and nearest value of Re are utilized as an initial guess. The radial-velocity profiles obtained by the present formulation for various Reynolds numbers using 51 G-L points are plotted in Figure 1. The computed results at $Re = 5000$ are compared to those obtained using (39); good agreement can be seen. When the Reynolds number increases, the velocity magnitude becomes nearly constant except near the plate walls, forming boundary layers of thickness $O(\sqrt{\alpha/Re})$ (Figure 1).

4.2.3 Eigenvalue problem - Free vibration of a uniform beam

The PIF is further verified through the solution of fourth-order eigenvalue problems subject to various types of boundary conditions. Consider the free lateral vibration of a uniform beam. The non-dimensional governing equation can be written as

$$\frac{d^4\phi}{dx^4} = \lambda\phi, \qquad 0 \leq x \leq 1, \tag{40}$$

and the boundary conditions are given by

$$\phi(0) = \phi'(0) = \phi(1) = \phi'(1) = 0, \quad \text{for a clamped-clamped beam (CC)}, \tag{41}$$

$$\phi(0) = \phi'(0) = \phi(1) = \phi''(1) = 0, \quad \text{for a clamped-hinged beam (CH)}, \tag{42}$$

$$\phi(0) = \phi''(0) = \phi(1) = \phi''(1) = 0, \quad \text{for a highed-hinged beam (HH)}, \tag{43}$$

where λ is the eigenvalue and ϕ is the eigenfunction. Exact solutions are found by solving the frequency equations

$$\cos(\lambda)\cosh(\lambda) = 1, \text{ (CC)}, \tag{44}$$

$$\tan(\lambda) - \tanh(\lambda) = 0, \text{ (CH)}, \tag{45}$$

$$\sin(\lambda) = 0, \ \lambda = n\pi, \text{ (HH)}. \tag{46}$$

Discretizing (40) at the whole set of G-L points and implementing the boundary conditions (41), (42) or (43) constitute the following two subsets of equations

$$\mathbf{Aa} - \lambda^4 \mathbf{Ba} = \mathbf{0}, \tag{47}$$

$$\mathbf{Ca} = \mathbf{0}, \tag{48}$$

or

$$(\mathbf{A}_1, \mathbf{A}_2)(\mathbf{a}_1, \mathbf{a}_2)^T - \lambda^4 (\mathbf{B}_1, \mathbf{B}_2)(\mathbf{a}_1, \mathbf{a}_2)^T = \mathbf{0}, \tag{49}$$

$$(\mathbf{C}_1, \mathbf{C}_2)(\mathbf{a}_1, \mathbf{a}_2)^T = \mathbf{0}, \tag{50}$$

where $\mathbf{A}_1$ and $\mathbf{B}_1$ are matrices of dimension $(N+1) \times (N+1)$, $\mathbf{A}_2$ and $\mathbf{B}_2$ of $(N+1) \times 4$, $\mathbf{C}_1$ of $4 \times (N+1)$, $\mathbf{C}_2$ of 4×4, $\mathbf{a}_1$ of $1 \times (N+1)$, and $\mathbf{a}_2$ of 1×4. After performing some algebraic manipulation, the above system of equations takes the form

$$[(\mathbf{A}_1 - \mathbf{A}_2\mathbf{C}_2^{-1}\mathbf{C}_1) - \lambda^4(\mathbf{B}_1 - \mathbf{B}_2\mathbf{C}_2^{-1}\mathbf{C}_1)]\mathbf{a}_1^T = \mathbf{0}. \tag{51}$$

A simple coordinate transformation ($[0,1] \rightarrow [-1,1]$) is carried out. Results concerning λ_k, $k = 1, \cdots, 5$, are shown in Table 4. Very accurate results and fast convergence are achieved. For example, the percentage errors for the case of a hinged-hinged beam using 18 grid points are 2.8×10^{-14}, 1.4×10^{-14}, 4.5×10^{-12}, 3.7×10^{-10} and 1.3×10^{-7}% for $\lambda_1, \cdots, \lambda_5$, respectively.

4.3 Sixth-order eigenvalue problem - Free vibration of a ring

The vibrational behaviour of a ring-like structure governed by a sixth-order ODE [6,7] is considered in this section. A ring has rectangular cross-sections of constant width and parabolically variable thickness. The case of normal, in-plane modes of vibration is studied here, where one disregards stretching in the axial direction.

4.3.1 A circular ring with supports

In this case, the non-dimensional governing equation is given by

$$\beta_1 v^{[6]} + \beta_2 v^{[5]} + \beta_3 v^{[4]} + \beta_4 v^{'''} + \beta_5 v^{''} + \beta_6 v^{'} - \Omega^2 \left(f v^{''} + f^{'} v^{'} - \pi^2 f v \right) = 0, \quad (52)$$

$$0 \leq \alpha \leq 1,$$

subject to the boundary conditions

$$v(0) = v^{'}(0) = v^{'''}(0) = 0, \quad v(1) = v^{'}(1) = v^{'''}(1) = 0,$$

where $v^{[q]} = d^q v / d\alpha^q$, v is the tangential displacement, α is the dimensionless variable, Ω is the dimensionless frequency and

$$\begin{aligned}
\beta_1 &= \phi/\pi^4, \quad \beta_2 = 3\phi^{'}/\pi^4, \quad \beta_3 = (2\phi/\pi^2) + (3\phi^{''}/\pi^4), \\
\beta_4 &= (4\phi^{'}/\pi^2) + (\phi^{'''}/\pi^4), \quad \beta_5 = \phi + (3\phi^{''}/\pi^2), \quad \beta_6 = \phi^{'} + (\phi^{'''}/\pi^2), \\
\phi &= [f(\alpha)]^3, \quad f(\alpha) = -4(r-1)\alpha^2 + 4(r-1)\alpha + 1,
\end{aligned}$$

in which r is the variable related to the thickness of the cross-section of the ring. The variable coefficients in (52) involve sixth-order polynomials in α. The solution procedure for this problem is similar to that for the previous problem and therefore

is omitted here for brevity. Six data sets, $\{7, 9, \cdots, 17\}$ G-L points, are employed. The fundamental frequencies obtained are listed in Table 5. The corresponding values predicted by the optimized Rayleigh-Ritz method [6] and the GDQR method [7] are also given for comparison purpose. They are in good agreement. The present method achieves highly accurate results using considerably small numbers of grid points. For $r = 1.5$, at least 4 significant digits remain constant when $(N+1) \geq 13$.

4.3.2 A completely free ring

In this case, the non-dimensional governing equation is given by

$$\beta_1 v^{[6]} + \beta_2 v^{[5]} + \beta_3 v^{[4]} + \beta_4 v''' + \beta_5 v'' + \beta_6 v' - \Omega^2 \left(f v'' + f' v' - \pi^2 f v/4 \right) = 0, \tag{53}$$

$$0 \leq \alpha \leq 1,$$

subject to the boundary conditions

$$\begin{aligned} v(0) &= v''(0) = 0, \quad \phi'(0) \left[v'(0) + 4v'''(0)/\pi^2 \right] + 4\phi(0) v^{[4]}(0)/\pi^2 = 0, \\ v(1) &= v''(1) = 0, \quad \phi'(1) \left[v'(1) + 4v'''(1)/\pi^2 \right] + 4\phi(1) v^{[4]}(1)/\pi^2 = 0, \end{aligned}$$

where

$$\begin{aligned} \beta_1 &= 16\phi/\pi^4, \quad \beta_2 = 48\phi'/\pi^4, \quad \beta_3 = (8\phi/\pi^2) + (48\phi''/\pi^4), \\ \beta_4 &= (16\phi'/\pi^2) + (16\phi'''/\pi^4), \quad \beta_5 = \phi + (12\phi''/\pi^2), \quad \beta_6 = \phi' + (4\phi'''/\pi^2), \\ \phi &= [f(\alpha)]^3, \quad f(\alpha) = -(r-1)\alpha^2 + 2(r-1)\alpha + 1. \end{aligned}$$

Five data sets, $\{5, 7, \cdots, 13\}$ G-L points, are employed. Table 6 displays the fundamental frequencies obtained by the present method together with those obtained by

the GDQR [7] and Rayleigh-Ritz [6] methods, where good agreement can be seen. Highly accurate results are achieved. For $r = 1.5$, at least 4 significant digits remain constant when $(N + 1) \geq 9$.

4.4 Eighth-order boundary-value problem

The governing equation and boundary conditions are, respectively, given by

$$\begin{aligned} &\frac{d^8u}{dx^8} = 7!\left[\exp(-8u) - \frac{2}{(1+x)^8}\right], \qquad a = 0 \leq x \leq b = \sqrt{e} - 1, \qquad (54)\\ &u(a) = 0,\ u(b) = 1/2,\\ &u^{[2i]}(a) = -(2i-1)!,\ u^{[2i]}(b) = -(2i-1)!e^{-i}, \quad i = 1, 2, 3, \end{aligned}$$

for which the exact solution is $u_e = \ln(1 + x)$. This nonlinear problem is taken from [10]. A Picard-type iteration is employed to render the nonlinear term linear. Eleven data sets, $\{6, 8, \cdots, 26\}$ G-L points, are employed. For this high-order problem, the condition numbers of the system matrix obtained by the CA2 and CA3 are very large (Table 7). It is remarkable that the condition numbers obtained for the PIF case only have the order of 10^4 for all the data sets. The relative L_2 errors are of $O(10^{-3}) - O(10^{-6})$, $O(10^{-4}) - O(10^{-9})$ and $O(10^{-6}) - O(10^{-16})$ for the CA2, CA3 and PIF, respectively; the PIF is far superior to the CA2 and CA3.

4.5 Twelfth-order boundary-value ODE

This problem is taken from [11], where the governing equation is

$$\frac{d^{12}u}{dx^{12}} = 11!\left[\exp(-12u) - \frac{2}{(1+x)^{12}}\right], \qquad a = 0 \leq x \leq b = e^{1/3} - 1, \qquad (55)$$

and the boundary conditions are

$$u(a) = 0,\ u(b) = 1/3,$$
$$u^{[2i]}(a) = -(2i-1)!,\ u^{[2i]}(b) = -(2i-1)!e^{-2i/3}, \quad i = 1, \cdots, 5,$$

for which the exact solution is $u_e = \ln(1+x)$. For this very high-order problem, the two approaches CA2 and CA3 fail to obtain a converged solution since their matrices are close to singular; for example, at $(N+1) = 4$, the conditioning of the system of the CA3 is already up to 2.77×10^{16}. Table 8 presents the conditioning of the system and the accuracy of the solution obtained by the PIF; an exponential rate of convergence is achieved.

5 CONCLUDING REMARKS

This paper presents a new Chebyshev spectral collocation method for directly solving high-order ODEs. The Chebyshev expressions representing the dependent variable and its derivatives are constructed through an integration process. This use of integration provides an effective way to implement the multiple boundary conditions, without the need to introduce fictitious points or the need to reduce the number of nodes used for discretizing the ODE. It works in a similar fashion for different types of the boundary condition and different orders of the ODE. The proposed method appears to be particularly well suited to problems governed by very high-order ODEs. Numerical results show that its performance is superior to those of conventional methods in terms of the conditioning of the system, accuracy and convergence rate.

ACKNOWLEDGEMENTS

The author would like to thank the referees for their helpful comments.

REFERENCES

1. Gottlieb D, Orszag SA. *Numerical Analysis of Spectral Methods: Theory and Applications*. SIAM: Philadelphia, 1977.

2. Canuto C, Hussaini MY, Quarteroni A, Zang TA. *Spectral Methods in Fluid Dynamics*. Springer-Verlag: New York, 1988.

3. Fornberg B. *A Practical Guide to Pseudospectral Methods*. Cambridge University Press: Cambridge, 1998.

4. Trefethen LN. *Spectral Methods in MATLAB*. SIAM: Philadelphia, 2000.

5. Peyret R. *Spectral Methods for Incompressible Viscous Flow*. Springer-Verlag: New York, 2002.

6. Gutierrez RH, Laura PAA. Vibrations of non-uniform rings studied by means of the differential quadrature method. *Journal of Sound and Vibration* 1995; **185(3)**: 507–513.

7. Wu TY, Liu GR. Application of generalized differential quadrature rule to sixth-order differential equations. *Communications in Numerical Methods in Engineering* 2000; **16**: 777–784.

8. Kelkar VS, Sewell RT. *Fundamentals of the Analysis and Design of Shell Structures*. Prentice-Hall: New Jersey, 1987.

9. Chandrasekhar S. *Hydrodynamic and Hydromagnetic Stability*. Oxford University Press: London, 1961.

10. Boutayeb A, Twizell EH. Finite-difference methods for the solution of special eighth-order boundary-value problems. *International Journal of Computer Mathematics* 1993, **48**: 63–75.

11. Boutayeb A, Twizell EH. Finite-difference methods for twelfth-order boundary-value problems. *Journal of Computational and Applied Mathematics* 1991, **35**: 133–138.

12. Mai-Duy N. Solving high order ordinary differential equations with radial basis function networks. *International Journal for Numerical Methods in Engineering* 2005, **62**: 824–852.

13. Bayliss A, Class A, Matkowsky BJ. Roundoff error in computing derivatives using the Chebyshev differentiation matrix. *Journal of Computational Physics* 1995, **116**(2): 380–383

14. Welfert BD. Generation of pseudospectral differentiation matrices I. *SIAM Journal on Numerical Analysis* 1997, **34**(4): 1640–1657.

15. Baltensperger R, Trummer MR. Spectral differencing with a twist. *SIAM Journal on Scientific Computing* 2003, **24**(5): 1465–1487.

16. Weideman JAC, Reddy SC. A MATLAB differentiation matrix suite. *ACM Transactions on Mathematical Software* 2000, **26**(4): 465–519.

17. Batchelor GK. *An Introduction to Fluid Dynamics*. Cambridge University Press: Cambridge, 1967.

18. McCartin BJ. A model-trust region algorithm utilizing a quadratic interpolant. *Journal of Computational and Applied Mathematics* 1998, **91**: 249–259.

Table 1: Second-order boundary-value problem: Conditioning and accuracy. Note that $a(b)$ means $a \times 10^b$.

$(N+1)$	Condition number			$Ne(u)$		
	CDF1	CDF2	PIF	CDF1	CDF2	PIF
10	2.08(3)	2.08(3)	5.30(1)	3.53(0)	3.53(0)	3.15(0)
15	1.39(4)	1.39(4)	6.16(1)	1.33(0)	1.33(0)	1.49(-2)
20	5.34(4)	5.34(4)	6.93(1)	2.64(-2)	2.64(-2)	6.02(-5)
25	1.50(5)	1.50(5)	7.62(1)	1.02(-4)	1.02(-4)	1.01(-7)
30	3.48(5)	3.48(5)	8.26(1)	4.71(-8)	4.71(-8)	1.54(-11)
35	7.07(5)	7.07(5)	8.85(1)	3.60(-11)	4.90(-11)	7.65(-12)
40	1.30(6)	1.30(6)	9.41(1)	1.14(-12)	2.54(-11)	4.43(-11)

Table 2: Fourth-order initial-value problem: Conditioning and accuracy (for the CA2 case, two interior points x_1 and x_{N-1} are put aside; for the CA3 case, two fictitious points are set to ± 1.1).

$(N+1)$	Condition number			$Ne(u)$		
	CDF		PIF	CDF		PIF
	CA2	CA3		CA2	CA3	
4	—	1.59(4)	1.21(2)	—	5.83(-3)	5.15(-5)
6	1.10(4)	2.47(5)	1.47(2)	1.03(-2)	7.10(-5)	4.32(-7)
8	1.39(5)	1.94(6)	1.70(2)	3.38(-4)	4.30(-7)	4.44(-10)
10	1.06(6)	9.08(6)	1.89(2)	3.82(-6)	1.52(-9)	5.11(-13)
12	5.58(6)	2.79(7)	2.07(2)	2.15(-8)	5.92(-12)	2.13(-15)
14	2.24(7)	6.02(7)	2.23(2)	4.78(-11)	7.66(-12)	5.93(-16)

Table 3: Fourth-order boundary value problem, Hamel flow, $Re = 0$: Conditioning and accuracy (for the CA2 case, two interior points x_1 and x_{N-1} are put aside; for the CA3 case, two fictitious points are set to ± 1.1).

$(N+1)$	Condition number			$Ne(u)$		
	CDF		PIF	CDF		PIF
	CA2	CA3		CA2	CA3	
5	4.68(2)	7.14(3)	2.50(2)	2.78(-2)	1.01(-3)	4.90(-5)
7	7.28(3)	7.01(4)	2.92(2)	3.22(-4)	5.49(-6)	1.64(-7)
9	5.17(4)	3.99(5)	3.30(2)	2.21(-6)	1.41(-8)	2.47(-10)
11	2.98(5)	1.46(6)	3.63(2)	6.65(-9)	2.75(-11)	2.82(-13)
13	1.29(6)	3.93(6)	3.94(2)	1.70(-11)	1.48(-13)	3.67(-16)
15	4.56(6)	7.82(6)	4.22(2)	2.31(-13)	4.88(-13)	1.55(-16)

Table 4: Fourth-order eigenvalue problem, free vibration of a uniform beam: eigenvalues obtained by the PIF.

$(N+1)$	λ_1(error %)	λ_2(error %)	λ_3(error %)	λ_4(error %)	λ_5(error %)
clamped-clamped beam					
8	4.7300(0.000)	7.8516(0.021)	11.1296(1.218)	13.9699(1.183)	24.9089(44.159)
10	4.7300(0.000)	7.8532(0.000)	10.9992(0.032)	14.0925(0.315)	18.1575(5.085)
12	4.7300(0.000)	7.8532(0.000)	10.9956(0.000)	14.1355(0.012)	17.3471(0.395)
14	4.7300(0.000)	7.8532(0.000)	10.9956(0.000)	14.1371(0.000)	17.2810(0.012)
16	4.7300(0.000)	7.8532(0.000)	10.9956(0.000)	14.1372(0.000)	17.2788(0.000)
18	4.7300(0.000)	7.8532(0.000)	10.9956(0.000)	14.1372(0.000)	17.2788(0.000)
clamped-hinged beam					
8	3.9266(0.000)	7.0683(0.003)	10.2606(0.494)	13.2950(0.425)	20.1161(21.964)
10	3.9266(0.000)	7.0686(0.000)	10.2111(0.008)	13.3384(0.100)	16.9003(2.466)
12	3.9266(0.000)	7.0686(0.000)	10.2102(0.000)	13.3514(0.003)	16.5196(0.158)
14	3.9266(0.000)	7.0686(0.000)	10.2102(0.000)	13.3518(0.000)	16.4940(0.003)
16	3.9266(0.000)	7.0686(0.000)	10.2102(0.000)	13.3518(0.000)	16.4934(0.000)
18	3.9266(0.000)	7.0686(0.000)	10.2102(0.000)	13.3518(0.000)	16.4934(0.000)
hinged-hinged beam					
8	3.1416(0.000)	6.2831(0.001)	9.4535(0.304)	12.4428(0.983)	19.0139(21.046)
10	3.1416(0.000)	6.2832(0.000)	9.4251(0.003)	12.5551(0.089)	16.0377(2.099)
12	3.1416(0.000)	6.2832(0.000)	9.4248(0.000)	12.5662(0.001)	15.7241(0.103)
14	3.1416(0.000)	6.2832(0.000)	9.4248(0.000)	12.5664(0.000)	15.7083(0.002)
16	3.1416(0.000)	6.2832(0.000)	9.4248(0.000)	12.5664(0.000)	15.7080(0.000)
18	3.1416(0.000)	6.2832(0.000)	9.4248(0.000)	12.5664(0.000)	15.7080(0.000)

Table 5: Sixth-order eigenvalue problem, free vibration of a non-uniform ring with constraints: fundamental frequencies.

	PIF						GDQR	Rayleigh-Ritz
r	7	9	11	13	15	17	[7]	[6]
1.0	2.2659	2.2667	2.2667	2.2667	2.2667	2.2667	2.2667	2.274
1.1	2.4134	2.4137	2.4137	2.4137	2.4137	2.4137	2.4137	2.416
1.2	2.5531	2.5569	2.5568	2.5568	2.5568	2.5568	2.5568	2.557
1.3	2.6690	2.6975	2.6966	2.6966	2.6966	2.6966	2.6966	2.697
1.4	2.7086	2.8387	2.8334	2.8334	2.8334	2.8334	2.8335	2.834
1.5	2.5572	2.9886	2.9673	2.9677	2.9677	2.9677	2.9678	2.970

Table 6: Sixth-order eigenvalue problem, free vibration of a non-uniform ring without constraints: fundamental frequencies.

	PIF					GDQR	Rayleigh-Ritz
r	5	7	9	11	13	[7]	[6]
1.0	2.6822	2.6833	2.6833	2.6833	2.6833	2.6833	2.687
1.1	2.8450	2.8452	2.8452	2.8452	2.8452	2.8452	2.846
1.2	3.0063	3.0062	3.0062	3.0062	3.0062	3.0062	3.006
1.3	3.1672	3.1665	3.1665	3.1665	3.1665	3.1665	3.167
1.4	3.3279	3.3262	3.3263	3.3263	3.3263	3.3263	3.326
1.5	3.4886	3.4857	3.4858	3.4858	3.4858	3.4858	3.486

Table 7: Eighth-order boundary-value problem: Conditioning and accuracy (for the CA2 case, 3 interior points adjacent to each boundary are put aside; for the CA3 case, fictitious points are set to $\{\pm 1.3, \pm 1.2, \pm 1.1\}$).

$(N+1)$	Condition number			$Ne(u)$		
	CDF		PIF	CDF		PIF
	CA2	CA3		CA2	CA3	
6	—	8.48(10)	1.51(4)	—	1.17(-5)	5.27(-6)
8	—	6.74(11)	1.74(4)	—	2.86(-7)	2.09(-8)
10	4.01(9)	3.39(12)	1.95(4)	1.70(-3)	7.92(-9)	2.58(-10)
12	3.80(10)	1.21(13)	2.13(4)	2.71(-4)	4.04(-8)	3.43(-12)
14	3.57(11)	1.20(14)	2.29(4)	2.79(-5)	2.92(-8)	5.04(-14)
16	2.76(12)	8.76(14)	2.45(4)	1.92(-6)	3.72(-7)	9.19(-16)
18	2.03(13)	3.87(15)	2.59(4)	2.09(-6)	6.16(-7)	2.61(-16)
20	1.17(14)	1.14(16)	2.73(4)	1.03(-6)	8.51(-6)	2.71(-16)
22	5.73(14)	2.45(16)	2.86(4)	1.04(-4)	2.92(-5)	2.95(-16)
24	2.41(15)	8.22(16)	2.98(4)	7.87(-5)	5.33(-5)	3.03(-16)
26	9.08(15)	4.33(17)	3.10(4)	3.11(-5)	5.97(-4)	4.07(-16)

Table 8: Twelfth-order boundary-value problem: Conditioning and accuracy of the PIF. Note that the CDF case fails to obtain a converged solution since the system matrices obtained are close to singular. For example, at $(N+1) = 4$, the conditioning of the system of the CA3 is up to 2.77×10^{16}.

$(N+1)$	Condition number	$Ne(u)$
4	4.18(8)	2.67(-5)
6	5.15(8)	2.22(-7)
8	5.95(8)	4.67(-10)
10	6.65(8)	4.55(-12)
12	7.27(8)	4.08(-14)
14	7.83(8)	5.57(-16)
16	8.36(8)	2.89(-16)

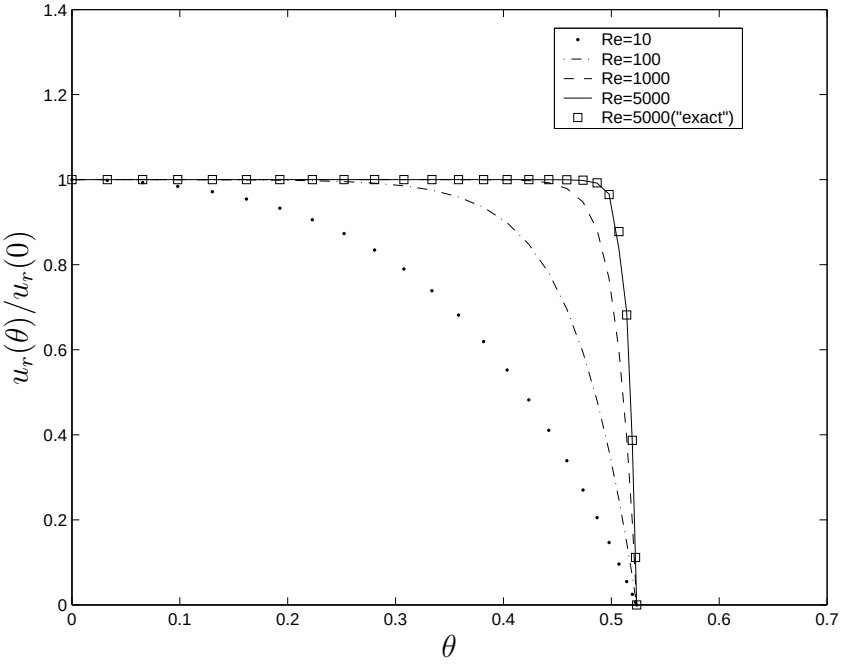

Figure 1: Fourth-order boundary-value problem, Hamel flow: the radial-velocity profiles for various values of the Reynolds number.